Effect of the Polymer Microstructure on the Behavior of Syndiotactic Polypropylene/Organophilic Layered Silicate Composites

H. Palza, A. Zurita

Departamento de Ingeniería Química y Biotecnología, Facultad de Ciencias Físicas y Matemáticas, Universidad de Chile, Beauchef 850, Santiago, Chile

Received 27 October 2010; accepted 7 May 2011
DOI 10.1002/app.34866
Published online 2 November 2011 in Wiley Online Library (wileyonlinelibrary.com).

ABSTRACT: Syndiotactic polypropylenes (sPPs) with several microstructures (i.e., syndiotacticities and molecular weights) and synthesized by means of two metallocenic catalysts were melt-blended with 1 and 3 wt % organophilic layered silicates in the presence of a compatibilizer. X-ray diffraction and transmission electron microscopy analysis showed that the clay was well dispersed in the composites, although the filler morphology depended on the polymer microstructure. Polypropylenes with low syndiotacticities and molecular weights presented the best clay dispersion. Nonisothermal differential scanning calorimetry analysis showed that the polymer microstructure and the clay content modified the thermal behavior of the composites. The compatibilizer and the clay acted as nucleant agents to increase the crystallization temperature of the matrix. Moreover, the double endothermic peak observed during heating scan and associated with the melt/recrystallization/remelt processes of the pure polymer matrix was reduced in the composites. With regard to the mechanical properties under tensile conditions, a synergic effect of the compatibilizer and the clay was observed. In particular, the addition of the compatibilizer alone was able to increase by about 20% the elastic modulus relative to the neat samples, whereas increases between 35 and 50% were measured when the clay was also added, depending on the polymer microstructure. Our results show that the microstructure of sPPs had strong effects on the behavior of its composites with clay in the presence of a compatibilizer. © 2011 Wiley Periodicals, Inc. J Appl Polym Sci 124: 2601–2609, 2012

Key words: nanocomposites; poly(propylene) (PP); syndiotactic

INTRODUCTION

The development of nanotechnology in polymer science has been strongly related to outstanding results of blending a polymer matrix with a nanoparticle to obtain a composite. The new composite era began with the results from the Toyota research group, in which they used organically modified clays as nanofillers because they showed that these layered silicates could improve the mechanical properties when they were exfoliated in a polymeric matrix.[1–3] Researchers later found other improvements, such as thermal degradation stabilities,[8–12] enhanced barrier properties,[13,14] melt fracture reduction,[15] among other improvements,[16,17] that were not easily improved with traditional microfillers could be further improved at low filler contents.[4–7] In the particular case of clay-based fillers, only a good interaction between the polymer and the silicate layers produces nanostructured composites. In this way, the final morphology in polyolefin/clay composites will be given by the specific interactions between the organoclay, the compatibilizer, and the polymer matrix.[4,16,18,19]

Polyolefin-based nanocomposites have been extensively studied in recent years, as these matrices are the largest volume polymers in the plastic industry today because of their excellent cost/performance value, low density, easy recyclability, and processability.[20] A great number of articles discussing isotactic polypropylene (iPP)/clay composites can be found elsewhere.[3,4,11,12,16,18,21] However, for syndiotactic polypropylenes (sPP), the numbers of articles is considerably lower, despite its good properties. sPP has, in general, higher impact resistance, adhesion to difference surfaces, clarity, heat sealability, tear strength, tolerance to high-energy radiation, oxidative degradation, and thermoplastic–elastomeric behavior than iPP.[22,23] Furthermore, sPP has a lower crystallinity and crystallization rate than iPPs; therefore, its mechanical properties are commercially insufficient; this makes the preparation of sPP/clay composites a viable alternative to overcome these limitations.

To our knowledge, there are few articles regarding sPP/clay composites. Mülhaupt et al.[24] studied sPP/clay composites based on a sample with a racemic

Correspondence to: H. Palza (hpalza@ing.uchile.cl).
Contract grant sponsors: Comisión Nacional de Investigación Científica y Tecnológica de Chile (CONICYT): project from Fondo Nacional de Desarrollo Científico y Tecnológico (FONDECYT Iniciación en Investigación 11075001).

pentad content of 78%, claiming a drastic raise in the Young's modulus value that was fivefold that of the neat polymer at a 20 wt % clay content. In these systems, the relevance of the compatibilizer based on grafted iPP on the mechanical properties of the composites was further concluded. Moreover, the crystallization temperature (T_c) was shifted to higher temperatures with an increase in the amount of compatibilizer.[24] A model based on core/shell-type nanoparticles containing clay as the core and a compatibilizer as the shell was able to represent the system. Vittoria et al.,[25] on basis of the same samples, found that the transport properties were shifted strongly with the presence of clay. In particular, the permeability and diffusion were drastically reduced, although this was independent of the clay content.[25] These nanocomposites were exfoliated at low clay contents and intercalated at high ones. Pucciariello et al.,[26] using the same sPP, found a strong influence of the compatibilizer on the crystallization rate of the matrix, which increased even more with the presence of the clay. Furthermore, the morphology and the crystallization processes in the composites were drastically affected by the presence of clay.[26] Fourier transform infrared spectroscopy analysis otherwise showed that the addition of clay resulted in a higher helical content in the composites than in the neat sPP matrix.[27] The presence of clay changed the conformation of the sPP during mechanical testing, increasing the tendency to return to the initial helical conformation after realization of the mechanical tension.[27] Dynamic mechanical analysis showed improved mechanical properties in the nanocomposites, especially at low temperatures.[27] Cerrada et al.[28] recently reported a stronger resistance of sPP/clay composites toward electroirradiation than of neat sPP, as shown by an analysis of T_c. The dimensional stability of sPP was preserved by the incorporation of a small amount of layered silicates. On the other hand, photooxidation studies on sPP/clay composites showed a clear prodegradation effect proportional to the amount of filler in the range between 1 and 10 wt %.[29]

Despite the relevant results found in the previously cited articles, all of these were focused in only one sPP matrix and lacked systematic studies on the effects of the polymer syndiotacticity on the main properties of the composites. Motivated by our recent results on the strong effect of polymer topology on the behavior of polypropylene (PP)/compatibilizer/clay nanocomposites,[30] this contribution is a first approach to understanding the relation between the polymer microstructure (i.e., syndiotacticities and molecular weights) and its properties in sPP/compatibilizer/clay composites. With two metallocenic catalysts, four different sPPs were synthesized, and their composites with commercials clay and compatibilizer were prepared and characterized.

EXPERIMENTAL

Materials

The montmorillonite sample was Cloisite 15A from Southern Clay Products, Inc. (Austin, Texas, US), with a cation-exchange capacity of 125 mequiv/100 g of clay. A commercial isotactic polypropylene grafted with maleic anhydride (PP$_g$MA; Aldrich) with a 0.6 mol % content was used as compatibilizer. The weight-average molecular weight (M_w) of the compatibilizer was 94 kg/mol with a polydispersity of 2.0, as measured by gel permeation chromatography (GPC).

The catalysts $(CH_3)_2C(Cp)(9\text{-Flu})ZrCl_2$ (Cat A) and $Ph_2C(Cp)(9\text{-Flu})ZrCl_2$ (Cat B), from Boulder Scientific, and the cocatalyst methylaluminoxane (MAO, St. Louis, Missouri, US), from Aldrich (10% w/v in toluene), were used as received. Toluene was distilled over sodium and distilled in an inert atmosphere, whereas the propene was purified by passage through three columns containing the BASF catalysts R3-11G and R3-12 and a 4-Å molecular sieve.

Polymerizations

All polymerizations were carried out in a 1-L Büchi glass reactor at a pressure of 2 bar and stirred at 1000 rpm for 30 min. First, the part of MAO dissolved in toluene was directly added to the reactor containing toluene under a nitrogen atmosphere. The Al/Zr molar ratio was set at 1000. At this point, the propylene was added to the reactor in the gas phase, and after 10 min, the solution in the reactor reached equilibrium concentration. Afterward, a certain amount of the commercial powder catalyst was also dissolved in toluene in the presence of MAO, and from this solution, the desired amount of catalyst was added to the reactor containing toluene under a nitrogen atmosphere. The total amount of toluene was set at 500 mL. All reactions and manipulations were carried out in an inert gas atmosphere with a standard Schlenk technique. When the reaction time elapsed, the polymer was coagulated with an excess of a methanol solution acidified with HCl, filtered, washed with further methanol and acetone, and then dried. The sPPs were synthesized with the two different metallocene/MAO catalytic systems. The sample sPPA1 was synthesized with Cat A at 50°C, and samples sPPB1, sPPB2, and sPPB3 were synthesized with Cat B at 50, 60, and 65°C, respectively.

Polymer characterization

The average molecular weights and molecular weight distributions were determined by GPC on a Waters Alliance GPC2000 system equipped with a differential optical refractometer (model 150 C, Milford, Massachusetts, US). A set of three columns of Styragel type HT (HT3, HT4, and HT6) was used with 1,2,4-

TABLE I
Main Characteristics of the Synthesized Syndiotactic Polymers

Sample	M_w (kg/mol)	Polydispersity	Syndiotacticity (% of racemic pentads in the polymer measured by 13C-NMR)	Crystallinity
sPPA1	90	1.6	74	0.23
sPPB1	300	1.8	77	0.19
sPPB2	220	1.8	72	0.14
sPPB3	180	1.7	66	0.11

trichlorobenzene as the solvent at 120°C. The analyses were calibrated with narrow-molecular-mass-distribution polystyrene standards. A set of standards (from 1,000 to 4,000,000 g/mol) were used to perform the calibration curve (elution time vs molecular weight).

Syndiotacticity was determined by ^{13}C-NMR, recorded at 125°C on a Varian Inova (Palo Alto, California, US) 300 instrument operating at 75 MHz.[31] Solutions of the polymer samples were prepared in *o*-dichlorobenzene and benzene-d6 (20% v/v) with 5-mm sample tubes. Details can be found elsewhere.[31] Under these conditions, the amount of regiodefects was measured as less than 3%, which is the current low value for metallocene catalysts as compared with other catalytic systems.[22,32,33] Moreover, the low signal-to-noise ratio in this area did not allow us to detect significant differences between the different samples. Because of the high stereodefects present in our samples (see Table I for details), the regiodefects were not considered in our analysis.

Nanocomposite preparation

For the preparation of the nanocomposites, first a master batch containing a mixture of Cloisite 15A and the compatibilizer with a 1 : 3 clay/compatibilizer weight ratio was prepared by a melt-mixing technique in a Brabender plasticorder internal mixer (Duisburg, Germany). The mixing conditions were 190°C, 110 rpm, and 10 min. The composites were also prepared with the Brabender plasticorder under the same conditions as those used for the preparation of the master batches by the mixture of predetermined amounts of the master batch, antioxidant, and neat polymer under a nitrogen atmosphere to obtain nanocomposites containing 1 and 3 wt % clay with 3 and 9 wt % compatibilizer, respectively.

Nanocomposite characterization

The nonisothermal crystallization exotherms and subsequent melting endotherms were obtained on a TA Instruments (New Castle, Delaware, US) DSC 2920 differential scanning calorimeter under an N_2 atmosphere to minimize thermal degradation. We started the experiment by heating each sample from 25 to 170°C at a heating rate of 40°C/min to delete its thermal history. To ensure complete melting, each sample was melt-annealed at 170°C for 5 min; afterward, it was cooled down at 10°C/min to 25°C. We then observed the subsequent melting behavior by reheating the sample to 170°C at a rate of 10°C/min.

Films with a thickness of 1 mm were prepared by the melting of the polymer in a hot press at 190°C. We then cooled the compression-molded film to 40°C in the compression press by running cold water through channels in the press plates. The films were kept at room temperature for 1 week and were then analyzed by X-ray diffraction or cut for mechanical property testing.

Wide-angle X-ray diffraction analysis was carried out with a Siemens (Munich, Germany) D-5000 diffractometer with Cu Kα = 1.54 Å and a step scan of 0.02° at room temperature. The mechanical properties were measured with an HP D500 dynamometer (HP Industry, Buenos Aires, Argentine) at a rate of 50 mm/min at 23°C and 30% relative humidity. Finally, transmission electron microscopy (TEM) measurements were made in a Philips model Tecnai 12 Biotwin at 80 kV. We obtained ultrathin sections of about 70 nm by cutting the samples with an Ultracut Reichert-Jung microtome equipped with a Diatome diamond knife.

RESULTS

sPPs

Table I shows the main characteristics of the different sPPs synthesized. By changing the reaction temperature, we obtained syndiotacticities between 66 and 77%, as measured by the racemic pentads from ^{13}C-NMR. From Table I, the strong effect of the syndiotacticity on the polymer crystallinity is clear; when this parameter was increased, the sample

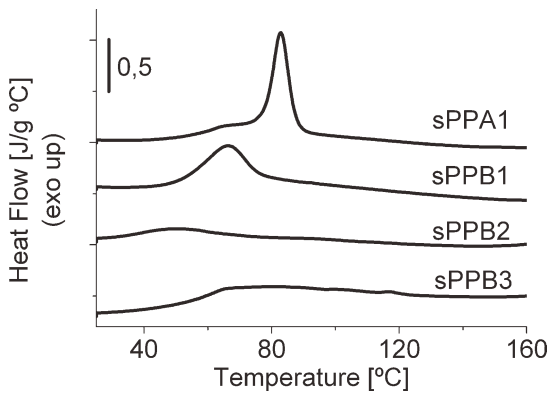

Figure 1 Cooling scan from melting for the different neat samples studied. The details are in Table I.

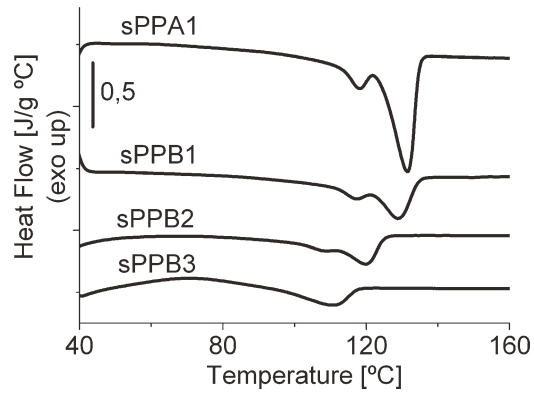

Figure 2 Heating scan for the different neat samples studied.

became more crystalline. However, the molecular weight was also another variable affecting crystallinity, as observed in a comparison of samples sPPA1 and sPPB2, which had similar syndiotacticities but different molecular weights.

Differential scanning calorimetry (DSC) analyses showed that the polymer microstructure had strong effects on the thermal behavior, as displayed in Figures 1 and 2 for the cooling and heating scans, respectively. Figure 1 clearly shows that T_c was drastically reduced when the syndiotacticity dropped, and in samples sPPB2 and sPPB3, only marginal exothermic processes during cooling were detected. By comparing the crystallization process of samples sPPA1 and sPPB2, we concluded the inverse relationship between the polymer crystallinity and molecular weight, whereas the syndiotacticity content was similar (Fig. 1). This confirmed the data from Table I. The effect of the polymer microstructure was even clearer in the analysis of the melting temperatures (T_m's) displayed during the heating scan (Fig. 2). These changes in T_m and T_c were explained by the fact that the stereodefects acted as comonomers being rejected from the polymeric crystals,[22,34–36] at least partially.[37] Flory, several decades ago, explained this phenomenon on the basis of thermodynamic reasons.[38] With the presence of a comonomer in the main chain, the lamellar thickness was not strictly controlled by the undercooling, but it was mainly dependent on the crystallizable sequence distribution. These sequences decrease when the defect content increases, forming lamellae with reduced lateral dimensions and poor faceting and modifying the whole crystallization process in the sample.[39,40] The increasing accumulation of the noncrystallizable species and sequences in the residual melt should be further considered to result in a systematic depression of T_m, similar to Raoult's law.[41,42]

Another characteristic of these samples was the presence of a double melting peak, which was more evident in the samples with low syndiotacticities.[22,43–47] This phenomenon is associated with melt/recrystallization/remelt (MRCRM) processes.[44] A nonreversing exothermic peak found in temperature-modulated DSC analysis confirmed this model.[47] Except for the sPPB3 sample, which had the lowest syndiotacticity, all of the samples presented MRCRM processes. Details can be found in ref. [47].

Morphology of the composites

The aforementioned samples were used to prepare composites with clay in the presence of a compatibilizer based on a grafted iPP. The d_{001} clay interlayer distance in the composites and in the master batch were measured by an X-ray diffraction technique. This gap between silicate layers from the clay is a good parameter for roughly quantifying the intercalated or exfoliated state of the clay in a polymer.[48] As reported previously for similar systems, the master batch did not present a relevant change in the interlayer distance (details in ref. [19]). However, a different tendency was observed in the composites. Figure 3 displays the X-ray diffractions of composites having 3 wt % clay and the pure organoclay. The composites presented an intercalated state, as the main diffraction peak was shifted to lower angles in all of the samples. This intercalated state and the good dispersion of the filler in the composites was confirmed by TEM, as displayed in Figure 4 for some representative samples. It was noteworthy that the final morphology, as estimated by X-ray diffraction, depended on the microstructure of the polymer. The sample with the highest syndiotacticity and molecular weight (sPPB1) presented a well-defined diffraction peak at $2\theta = 2.4°$ (3.68 nm); this indicated a clear intercalated morphology, as the original organoclay had a peak at $2\theta = 2.9°$ (3.04

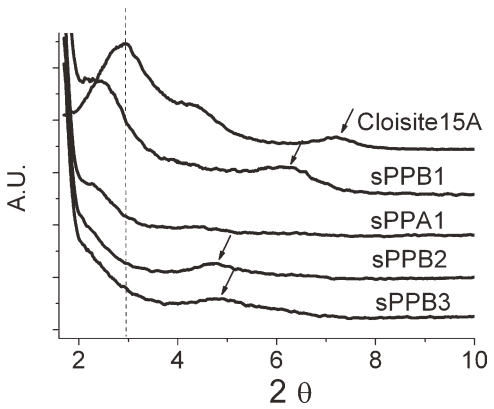

Figure 3 X-ray diffractions at low angles of the nanocomposites with 3 wt % clay. It is also shown the diffraction of the pure organically modified clay used. A dashed line represents the main diffraction peak of the clay. The arrows show the position of the secondary diffraction peak. A.U.: arbitrary units.

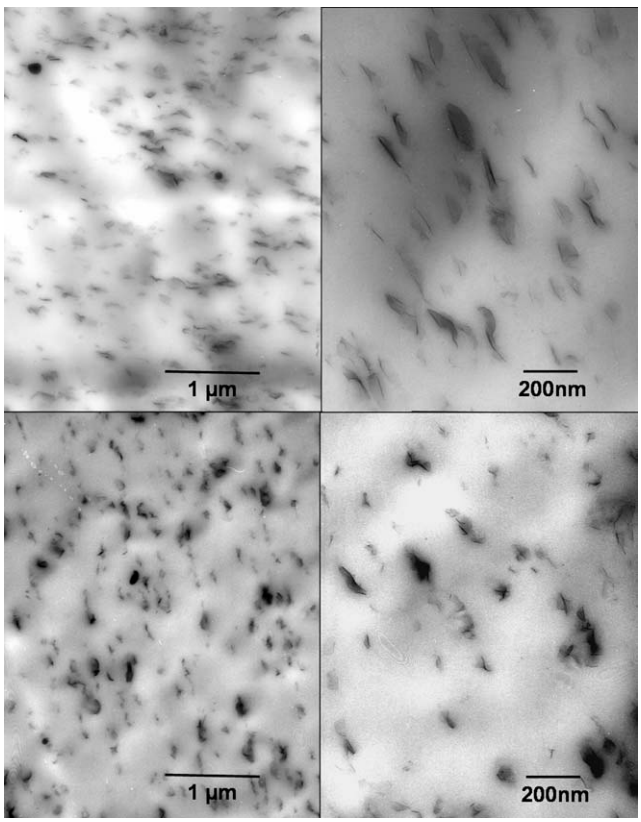

Figure 4 TEM images of some representative sPP/clay composites: (top) sPPA1 and (bottom) sPPB2.

nm). sPPA1, having higher stereodefects and a lower molecular weight than sPPB1, presented the same diffraction peak but with decreased intensity, which indicated a degree of exfoliation. When the syndiotacticity and molecular weight were decreased even more, a better intercalated state was found in the composites, as the diffraction peaks shifted to lower angles and became more diffuse. In particular, composites based on samples sPPB2 and sPPB3 only presented the secondary diffraction peak of the d_{001} peak located at an angle lower than the resolution of the equipment. By observing this secondary peak (see arrows in Fig. 3), we could evaluate the morphology of the composites. Therefore, the polymer microstructure strongly affected the clay morphology in the composites. In particular, by decreasing the stereoregularity and the molecular weight, we facilitated the intercalation.

The mechanisms for understanding the polymer melt intercalation process can be separated in two:[30,49] those based on chemical interactions between the clay and the polymer[49,50] and those based on mechanical or physical interactions, such as the peeling, diffusion, or breakup mechanisms.[49] Although both approaches are not independent, in our analysis, we assumed that the physical processes drove the final clay morphology in the nonpolar polymer. The breakup mechanism states that clay exfoliation is improved when the viscosity (or molecular weight) of the matrix is increased, as was reported by analysis of the hydrodynamic and stretching forces in platelets particles immersed in a polymeric fluid.[48] The diffusion mechanism, otherwise, is independent of the stress field, as the diffusion of the polymer from the edge to the center of the clay is the relevant phenomenon.[48,49] By facilitating the diffusion processes, for example, decreasing the viscosity of the matrix, one improves the exfoliation, as reported for PP/clay nanocomposites.[18,21,30] Therefore, the effect of the viscosity on the clay intercalation will depend on the specific mechanism explaining the system.[30]

The PP microstructure dramatically modifies its viscosity, conformation, coil dimensions, and thermodynamic properties.[51] It is well known that sPP displays a marked chain flexibility compared with iPP; this results in a lower molecular weight between entanglement couplings.[52] The different melt chain conformation of sPP explained the values of molecular weight between entanglement couplings, which was around 70% less than those reported for atactic or iPPs[53] and changes in compatibility with other polymer matrices.[54] Noteworthy, sPP displayed a larger viscosity than iPP at the same molecular weight.[55] In this way, the viscosity of the sPP could be reduced by one order of magnitude by an increase in the stereodefects because of changes in the chain stiffness.[55] The same effect was observed with a decrease in the polymer molecular weight.[55]

Therefore, on the basis of the aforementioned and despite the fact that the three physical mechanisms (breakup, peeling, and diffusion) could have been simultaneously present in our process, we concluded that the diffusion mechanism properly represented our experimental findings. With a decrease in the polymer syndiotacticity or its molecular weight, as in sPPB2 and sPPB3, the viscosity decreased, and the polymer diffusion toward the clay galleries was facilitated; this improved the intercalation state, as our results confirmed. Similar results were recently reported with increases in the amount of short-chain branching in iPPs.[30]

sPP has been studied extensively in materials science because of its complex polymorphism with practical consequences, such as high nonlinear reversible deformation.[22] sPP displays at least four limited/ordered crystal structures or polymorphisms, depending on the crystallization conditions and the stereoregularity of the polymer.[22] Form I is the most stable crystalline structure, and it is characterized by one orthorhombic unit cell with chains in the s(2/1)2 antichiral helical conformation, having either ordered or disordered structures. The metastable form II has a similar structure as form I but with an isochiral conformation, whereas forms III and IV present chains in the transplanar and $(T_6G_2T_2G_2)_n$ conformations, respectively.[22,34]

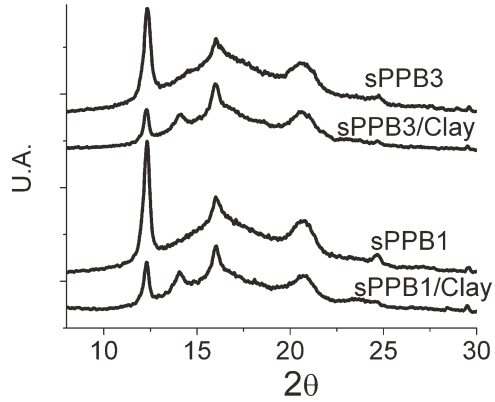

Figure 5 X-ray diffractions of some representative nanocomposites with 3 wt % clay and their neat matrices. The other samples are not shown as they displayed the same tendency. The (010) reflection at $2\theta = 15.9°$ confirmed the disordered form I structure of the samples. U.A.: arbitrary units.

All our samples and their composites displayed a disordered form I polymorph, as shown in Figure 5, where some representative X-ray diffractions from sPP and its composites are given. The neat polymers presented the (010) reflection at $2\theta = 15.9°$, whereas the (211) reflection at $2\theta = 18.8°$ was completely absent; this confirmed the disordered form I structure. In a previous article, it was found that a larger number of defects was needed to find the form II in the as-prepared samples.[47] The composites otherwise presented the same diffraction pattern as the pure polymer; this showed that the presence of clay was not able to modify the crystalline structure of the sPP. The peak observed in the composites at $2\theta = 14.1°$ (see Fig. 5) was due to the compatibilizer, and it did not represent any change in the crystalline structure of the pure matrix.

Thermal properties of the nanocomposites

Regarding the nonisothermal crystallizations of the composites, Figures 6–8 present examples of the complex behavior found by DSC for the sPPA1, sPPB1, and sPPB3 matrices, respectively. Composites based on polyolefins are three-phased systems compounded by the polymer matrix, the compatibilizer, and the clay; therefore, the drastic effect that the compatibilizer could have on the polymer matrix should be considered.[30] In this way, blends of sPP with 9 wt % compatibilizer but without clay were prepared and characterized by DSC.

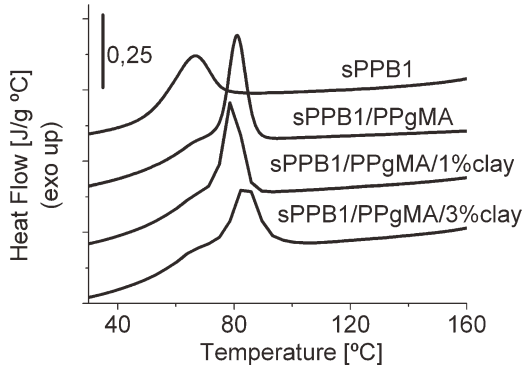

Figure 7 Cooling scan from melting for sPPB1, its blend, and its nanocomposites with 1 and 3 wt % clay.

The crystallization process of the three-phased nanocomposites was complex and depended strongly on the characteristic of the matrix. This complexity was related with the fact that the matrix crystallization could depend of the compatibilizer and the clay. Moreover, the crystallization of the compatibilizer could also have been modified in the system. As discussed later, our results show that matrices of high viscosities and low stereodefects inhibited the crystallization of the compatibilizer in the blend, although the presence of PPgMA could act as a nucleating agent for the same kind of matrices. Moreover, clay could also act as a nucleating agent of both polymers, even promoting a phase separation, depending on their characteristics.

Figure 6 shows that the crystallizations of sPPA1 ($T_c = 78°C$) and the compatibilizer ($T_c = 119°C$)

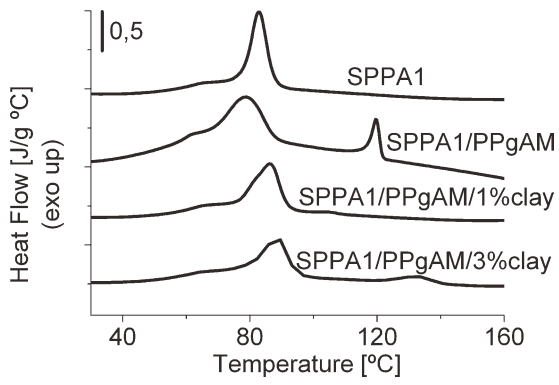

Figure 6 Cooling scan from melting for sPPA1, its blend, and its nanocomposites with 1 and 3 wt % clay. The exothermic peak at 120°C corresponded to the compatibilizer.

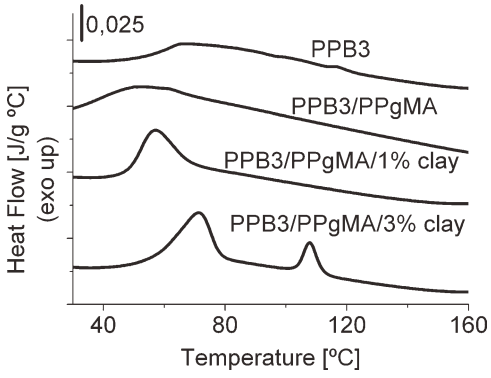

Figure 8 Cooling scan from melting for sPPB3 sample (see Table 1 for details), its blend, and its nanocomposites with 1 and 3 wt % clay. The exothermic peak at 110°C corresponded to the compatibilizer.

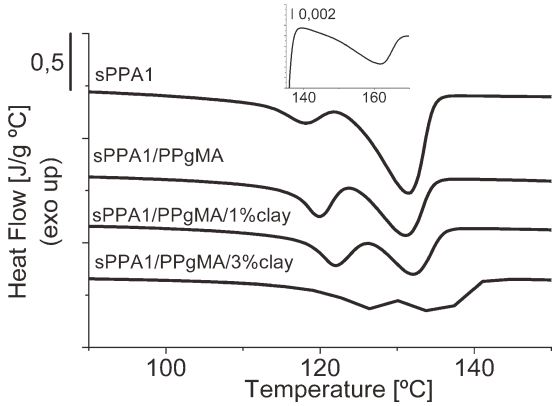

Figure 9 Heating scan for sPPA1, its blend, and its nanocomposites with 1 and 3 wt % clay.

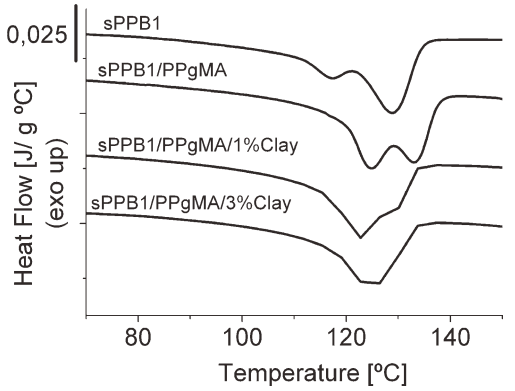

Figure 10 Heating scan for sPPB1, its blend, and its nanocomposites with 1 and 3 wt % clay.

were independent in the blend, showing a phase separation between both PPs, as reported elsewhere.[22,24,56,57] When the clay was added, the crystallization of the compatibilizer disappeared, and the T_c of the composite was higher than that of the neat matrix (T_c = 86°C); this showed a nucleating effect. In sPPB1 (Fig. 7), the crystallization of the compatibilizer was not detected in the blend, although T_c of the matrix increased 13°C and the process was narrowed, as found previously; this showed that the compatibilizer could act as a nucleating agent.[28] This matrix presented the largest molecular weight and the lowest stereodefects; this indicated a high viscosity in the melt, as explained earlier. Therefore, this high viscosity could inhibit the crystallization of the compatibilizer under these crystallization conditions. The presence of clay otherwise did not change the T_c of the blend. The inhibition of crystallization of the compatibilizer by high-viscous matrices (or a polymer of low stereodefects) and its nucleating effect was confirmed by observation of the behavior of sPPB3, as displayed in Figure 8. sPPB3 was not able to crystallize on cooling but presented a broad and small exothermic peak (T_c = 54°C) when the compatibilizer was added. With the further addition of 1 wt % clay, the exothermic peak of the matrix was narrowed and showed some nucleating effect. Nevertheless, with 3 wt % clay, the matrix not only displayed an increased T_c of 71°C, but a crystallization related to the compatibilizer (T_c = 108°C) also appeared. With the presence of clay, the maleic anhydride groups from the compatibilizer had a higher tendency to interact with the clay than with the sPP, and a phase separation occurred, as the core/shell model states.[24] Furthermore, there was a synergic effect between the clay and the compatibilizer that increased the crystallization processes of the matrix, as observed in this sample. In this case, two exothermic peaks appeared at a high concentration of filler, as displayed in Figure 8. The same behavior was observed in composites based on sPPB2 (results not shown). The aforementioned confirmed that the interactions between sPP and iPP depended on the polymer microstructure.[22,58]

Figures 9–11 present the melting behavior of the composites based on sPPA1, sPPB1, and sPPB3, respectively. The most important effect was associated with the MRCRM process, as observed by the changes in the relative intensities of the double melting peak. In general, the presence of the compatibilizer increased the low endothermic peak, which was even more pronounced when the clay was added. It is well known that MRCRM processes are reduced with high heating rates, as the time available for the diffusion of the molecular segments onto the growing recrystallizing lamellae is shorter when the high-temperature melting peak is reduced.[44,48] Therefore, the presence of both clay and compatibilizer could restrict the motion of the syndiotactic polymers chains or segments, which would reduce or slow down their ability to recrystallize during heating.[28] The same conclusion was stated previously on the basis of the crystallinity of the composites.[26]

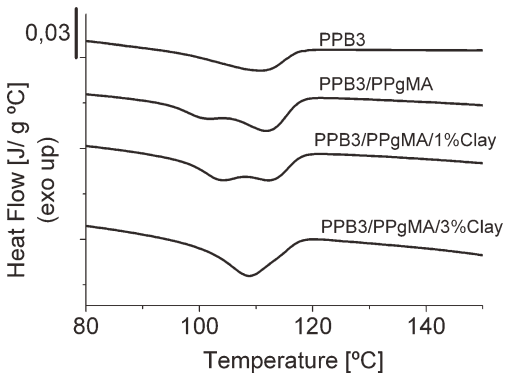

Figure 11 Heating scan for sPPB3 sample (see Table 1 for details), its blend, and its nanocomposites with 1 and 3 wt % clay.

TABLE II
Main Mechanical Properties under Tensile Conditions of the Neat Polymers, Their Blends with the Compatibilizer, and Their Nanocomposites with 1 and 3 wt % Clay

	E (MPa)	ε_y (%)	σ_y (MPa)	ε_{break} (%)
sPPA1	266 ± 53	9.5 ± 0.6	16.8 ± 0,2	38 ± 3
sPPA1/PPgMA	322 ± 81	9.7 ± 0.4	18.5 ± 0,8	12 ± 2
sPPA1/PPgMA/1% clay	357 ± 62	9.7 ± 0.9	18.6 ± 0,4	13 ± 3
sPPA1/PPgMA/3% clay	396 ± 78	6.9 ± 1.4	15.8 ± 0,3	7 ± 1
sPPB1	229 ± 36	11.0 ± 0,5	14.8 ± 0,2	217 ± 57
sPPB1/PPgMA	272 ± 9	11.5 ± 0,3	16.8 ± 0,4	673 ± 34
sPPB1/PPgMA/1% clay	309 ± 77	11.3 ± 0,5	15.9 ± 0,4	363 ± 13
sPPB1/PPgMA/3% clay	320 ± 83	10.1 ± 0,9	16.8 ± 0,9	301 ± 124
sPPB2	228 ± 16	11.4 ± 0,2	14.7 ± 0,1	481 ± 126
sPPB2/PPgMA	271, ± 26	9.8 ± 0,7	15.1 ± 1,2	421± 26
sPPB2/PPgMA/1% clay	282 ± 53	11.2 ± 0,7	12.9 ± 0,3	>600
sPPB2/PPgMA/3% clay	296 ± 80	11 ± 1	14.8 ± 0,6	13 ± 2
sPPB3	189 ± 24	11.1 ± 0,5	11.9± 0,3	422 ± 260
sPPB3/PPgMA	224 ± 14	11.4 ± 0,4	11.3 ± 0,5	662 ± 79
sPPB3/PPgMA/1% clay	233 ± 47	11.5 ± 0,4	13.5 ± 0,2	618 ± 67
sPPB3/PPgMA/3% clay	255 ± 30	10.4 ± 0,6	13.8 ± 0,3	456 ± 302

E: Elastic modulus; ε_y: yield strain; σ_y: yield strength; ε_{break}: elongation to break.

Mechanical properties of the nanocomposites

Table II presents a summary of the main mechanical properties of the neat matrices, their blends with the compatibilizer, and their composites with 1 and 3 wt % clay, as measured by tensile tests. By comparing Tables I and II, we concluded the direct relationship between the crystallinity of the sample and the elastic modulus, as previously reported for other polyolefinic matrices.[59–61] Therefore, as discussed previously, the polymer molecular weight and syndiotacticity, both affecting the crystallinity (see Table I), were two variables that affected the mechanical behavior of the polymer. For example, sPPB1 displayed the highest syndiotacticity, but it had a lower elastic modulus than sPPA1 because of its high-molecular-weight; this decreased the crystallinity.

Similar to the thermal properties, the presence of the compatibilizer was able to increase the elastic modulus of the neat matrix, raising its value around 20%. This increase in the elastic modulus was explained by the different stiffnesses of the matrices. As observed in Table II, the sPP matrices had values around 300 MPa, whereas the compatibilizer had values that were higher than those of the matrix.[62,63] Regarding the plastic behavior, the blends presenting a reduced phase separation (as concluded by their crystallization behavior) displayed similar or even higher elongations at break than the neat polymers. In fact, the only blend that had a reduced elongation at break (with the experimental error taken into account) was based on sPPA1 and presented a clear phase separation with the compatibilizer (Fig. 6). With the presence of clay, the properties shifted even more, and the elastic modulus increased between 35 and 50%, depending of the polymer matrix. These increases were not as high as those previously reported by Kaempfer et al.,[24] but with the low clay content used here and the effect of the compatibilizer considered, our results had the same tendency. The elongation at break of the composites with 1 wt % clay increased relative to the neat samples, except for sPPA1; this was similar to the behavior of the blends. With 3 wt % clay, this property depended on the phase separation of the sPP/compatibilizer system, as composites presenting phase separation on DSC (sPPB2 and sPPB3) showed lower elongations at break than the neat sample or composites with 1 wt % clay. In Table II, it is also shown that the experimental error of the samples increased when the clay was added. This could have indicated an irregular distribution of clay morphologies in the polymer matrix.

CONCLUSIONS

By using two metallocenic catalysts, we synthesized a set of sPPs, and their nanocomposites with 1 and 3 wt % clay with a compatibilizer based on an iPP were studied. The composites displayed a good filler dispersion and intercalated states, as observed by X-ray diffraction and TEM. In general, matrices with high stereodefects and lower molecular weights presented better morphologies, as quantified by X-ray diffraction. All of the sPPs displayed the same crystalline structure without any relevant modification when the clay and the compatibilizer were added. DSC analysis showed that the polymer microstructure and the content of clay highly affected the phase separation between the matrix and the

compatibilizer. In general, the compatibilizer acted as a nucleating agent, although the clay could further modify these processes. With regard to the melting behavior, the MRCRM processes were inhibited by the presence of both the compatibilizer and the clay. In particular, the low endothermic peak in the nanocomposites was raised relatively because of restrictions on the recrystallization processes because of the clay. Finally, the mechanical properties under tensile conditions showed that the compatibilizer was able to increase by 20% the elastic modulus, whereas the clay raised this property up to 50%, depending on the matrix.

The authors thank R. Quijada for the support during this research.

References

1. Usuki, A.; Kojima, Y.; Kawasumi, M.; Okada, A.; Fukusihima, Y.; Kurauchi, T. T. J. Mater Res 1993, 8, 1179.
2. Kojima, Y.; Usuki, A.; Kawasumi, K.; Okada, A.; Kurauchi, T. T.; Kamigaito, O. J Polym Sci Part A: Polym Chem 1993, 31, 983.
3. Kawasumi, M.; Hasegawa, N.; Kato, M.; Usuki, A.; Okada, A. Macromolecules 1997, 30, 6333.
4. Ray, S.; Okamoto, M. Prog Polym Sci 2003, 28, 1539.
5. Podsiadlo, P.; Kaushik, A. K.; Arruda, E. M.; Waas, A. M.; Shim, B. S.; Xu, J.; Nandivada, H.; Pumplin, B. G.; Lahann, J.; Ramamoorthy, A.; Kotov, N. A. Science 2007, 318, 80.
6. Liff, S. M.; Kumar, N.; Mckinley, G. H. Nat Mater 2007, 6, 76.
7. Manias, E. Nat Mater 2007, 6, 9.
8. Leszczynska, A.; Njuguna, J.; Pielichowski, K.; Banerjee, J. R. Therm Acta 2007, 454, 1.
9. Guo, B.; Jia, D.; Cai, C. Eur Polym J 2004, 40, 1743.
10. Qin, H.; Zhang, S.; Zhao, C.; Feng, M.; Yang, M.; Shu, Z.; Yang, S. Polym Degrad Stab 2004, 85, 807.
11. Zanetti, M.; Camino, G.; Reichert, P.; Mülhaupt, R. Macromol Rapid Commun 2001, 22, 176.
12. Palza, H.; Yazdani-Pedram, M. Macromol Mater Eng 2009, 295, 48.
13. Ciardelli, F.; Coiai, S.; Passaglia, E.; Pucci, A.; Ruggeri, G. Polym Int 2008, 57, 805.
14. Gusev, A. A.; Lusti, H. R. Adv Mater 2001, 13, 1641.
15. Palza, H.; Reznik, B.; Kappes, M.; Hennrich, F.; Naue, I. F. C.; Wilhelm, M. Polymer 2010, 51, 3753.
16. Paul, D. R.; Robeson, R. M. Polymer 2008, 49, 3187.
17. Palza, H.; Gutiérrez, S.; Delgado, K.; Salazar, O.; Fuenzalida, V.; Avila, J.; Figueroa, G.; Quijada, R. Macromol Rapid Commun 2010, 31, 563.
18. Vaia, R.; Giannelis, E. Macromolecules 1997, 30, 8000.
19. Palza, H.; Vergara, R.; Yazdani-Pedram, M.; Quijada, R. J Appl Polym Sci 2009, 112, 1278.
20. Chum, P. S.; Swogger, K. W. Prog Polym Sci 2008, 33, 797.
21. Gianelli, W.; Ferrara, G.; Camino, G.; Pellegatti, G.; Rosenthal, J.; Tromboni, R. C. Polymer 2005, 46, 7037.
22. De Rosa, C. D.; Auriemma, F. Prog Polym Sci 2006, 31, 145.
23. Portnoy, R. C.; Domine, J. D. Metallocene Based Polyolefins; Scheirs, J., Kaminsky, W., Eds.; Wiley: New York, 2000.
24. Kaempfer, D.; Thomann, R.; Mülhaupt, R. Polymer 2002, 43, 2909.
25. Gorrasi, G.; Tortora, M.; Vittoria, V.; Kaempfer, D.; Mülhaupt, R. Polymer 2003, 44, 3679.
26. Pucciariello, R.; Villani, V.; Guadagno, L.; Vittoria, V. Polym Eng Sci 2006, 46, 1433.
27. Gregoriou, V. G.; Kandilioti, G.; Bollas, S. T. Polymer 2005, 46, 11340.
28. Cerrada, M. L.; Rodríguez-Amor, V.; Perez, E. J Polym Sci Part B: Polym Phys 2007, 45, 1068.
29. Cómela, S.; Fledlerova, A.; Borsig, E.; Erler, J.; Mülhaupt, R. J Macromol Sci Part A: Pure Appl Chem 2007, 44, 1027.
30. Palza, H. Macromol Mater Eng 2010, 295, 492.
31. Simanke, A. G.; Mauler, R. S.; Galland, G. B. J Polym Sci Part A: Polym Chem 2002, 40, 471.
32. Lamberti, M.; Pappalardo, D.; Zambelli, A.; Pellecchia, C. Macromolecules 2002, 35, 658.
33. Lamberti, M.; Gliubizzi, R.; Mazzeo, M.; Tedesco, C.; Pellecchia, C. Macromolecules 2004, 37, 276.
34. De Rosa, C.; Auriemma, F.; Fanelli, E.; Talarico, G.; Capitani, C. Macromolecules 1997, 30, 4137.
35. Balbontin, G.; Dainelli, D.; Galimbert, M.; Paganetto, G. Macromol Chem 1992, 193, 693.
36. De Rosa, C.; Auriemma, F.; Vinti, V.; Galimberti, M. Macromolecules 1998, 31, 6206.
37. Auriemma, F.; De Rosa, C.; Corradini, P. Macromolecules 1993, 26, 5719.
38. Flory, P. J. J Am Chem Soc 1962, 84, 2857.
39. Alizadeh, A.; Richardson, L.; Xu, J.; McCartney, S.; Marand, H.; Cheung, Y. W.; Chum, S. Macromolecules 1999, 32, 6221.
40. Keesu, J.; Palza, H.; Quijada, R.; Alamo, R. G. Polymer 2009, 50, 832.
41. Alamo, R. G.; Mandelkern, L. Macromolecules 1991, 24, 6480.
42. Brune, D.; Bicerano, J. Polymer 2002, 43, 369.
43. Rodríguez-Arnold, J.; Zhang, A.; Cheng, S. Z. D.; Lovinger, A. J.; Hsieh, E. T.; Chu, P. Polymer 1994, 35, 1884.
44. Supaphol, P. J Appl Polym Sci 2001, 82, 1083.
45. Boor, J.; Youngman, E. A. J Polym Sci Polym Phys Ed 1965, 3, 577.
46. Youngman, E. A.; Boor, J. Macromol Rev 1967, 2, 33.
47. Vanegas, M. E.; Quijada, R.; Serafín, D.; Galland, G. B.; Palza, H. J Polym Sci Part B: Polym Phys 2008, 46, 798.
48. Bhattacharya, S. N.; Gupta, R. K.; Kamal, M. R. Polymeric Nanocomposites; Hanser: Munich, 2008.
49. Dennis, H. R.; Hunter, D. L.; Chang, D.; Kim, S.; White, J. L.; Cho, J. W.; Paul, D. R. Polymer 2001, 42, 9513.
50. Manias, E.; Touny, A.; Wu, L.; Strawhecker, K.; Lu, B.; Chung, T. C. Chem Mater 2001, 13, 3516.
51. Jones, T. D.; Chaffin, K. A.; Bates, F. S.; Annis, B. K.; Hagaman, E. W.; Kim, M. H.; Wignall, G. D.; Fan, W.; Waymouth, R. Macromolecules 2002, 35, 5061.
52. Suzuki, M.; Ali, M. A.; Okamoto, K.; Tanike, T.; Terano, M.; Yamaguchi, M. Adv Polym Technol 2009, 28, 185.
53. Eckstein, A.; Suhm, J.; Friedrich, C.; Maier, R. D.; Sassmannshausen, J.; Bochmann, M.; Mülhaupt, R. Macromolecules 1998, 31, 1335.
54. Yamaguchi, M.; Miyata, H. Macromolecules 1999, 32, 5911.
55. Rojo, E.; Muñoz, M. E.; Santamaria, A.; Peña, B. Macromol Rapid Commun 2004, 25, 1314.
56. Thomann, R.; Kressler, J.; Setz, S.; Wang, C.; Mülhaupt, R. Polymer 1996, 37, 2627.
57. Thomann, R.; Kressler, J.; Rudolf, B.; Mülhaupt, R. Polymer 1996, 37, 2635.
58. Maier, R. D.; Thomann, R.; Kressler, J.; Mülhaupt, R.; Rudolf, B. J Polym Sci Part B: Polym Phys 1997, 35, 1135.
59. Palza, H.; Lopez-Majada, J. M.; Quijada, R.; Pereña, J. M.; Benavente, R.; Perez, E.; Cerrada, M. L. Macromol Chem Phys 2008, 209, 2259.
60. Palza, H.; Lopez, J. M.; Quijada, R.; Benavente, R.; Perez, E.; Cerrada, M. L. Macromol Chem Phys 2005, 206, 1221.
61. Bensason, S.; Minick, J.; Moet, A.; Chum, S.; Hiltner, A.; Baer, E. J Polym Sci Part B: Polym Phys 1996, 34, 1301.
62. Szazdi, L.; Pukanszky, B., Jr.; Vancso, G.; Pukanszky, B. Polymer 2006, 47, 4638.
63. Chen, L.; Wong, S. C.; Pisharath, S. J Appl Polym Sci 2003, 88, 3298.